ASIAN JOURNAL OF PHARMACEUTICAL AND CLINICAL RESEARCH

INNOVARE ACADEMIC SCIENCES
Knowledge to Innovation

Vol 19, Issue 4, 2026

Online - 2455-3891
Print - 0974-2441

Research Article

BIOSYNTHESIS OF IRON OXIDE NANOPARTICLES USING *HYDROCOTYLE UMBELLATA L.* AND ITS ANTIDIABETIC AND ANTIOXIDANT ACTIVITY

SULOCHANA GOVINDHARAJ[1], KOHILA KALIMUTHU[2], KANISH S[1], RAJESHKUMAR SHANMUGAM[1]*

[1]Department of Anatomy, Nanobiomedicine Laboratory, Saveetha Medical College and Hospital, Saveetha Institute of Medical and Technical Sciences, Saveetha University, Chennai, Tamil Nadu, India. [2]Department of Obstetrics and Gynaecology, Saveetha Medical College and Hospital, Saveetha Institute of Medical and Technical Science, Saveetha University, Chennai, Tamil Nadu, India.
***Corresponding author: Rajeskumar Shanmugam; Email: rajeshkumars.sdc@saveetha.com**

Received: 05 January 2026, Revised and Accepted: 18 February 2026

ABSTRACT

Objectives: The objective of the present study was to synthesize iron oxide nanoparticles (Fe_2O_3 nanoparticles [NPs]) using Hydrocotyle umbellata L. through a biogenic approach and to evaluate their antidiabetic potential through α-amylase and α-glucosidase inhibitory assays, along with antioxidant activity using 2,2-Diphenyl-1-picrylhydrazyl (DPPH), H_2O_2, Ferric reducing antioxidant power (FRAP), 2,2'-azino-bis(3-ethylbenzothiazoline-6-sulfonic acid) ABTS, and nitric oxide scavenging assays.

Methods: Iron oxide nanoparticles were synthesized using H. umbellata L. extract and characterized by ultraviolet (UV)-visible spectroscopy, Fourier transform infrared spectroscopy, X-ray diffraction, and scanning electron microscopy analysis. The antioxidant efficacy of the synthesized nanoparticles was evaluated using DPPH, hydrogen peroxide (H_2O_2), FRAP, ABTS, and nitric oxide assays. Antidiabetic activity was assessed through α-amylase and α-glucosidase inhibitory assays at different concentrations (10–50 µg/mL), and results were compared with standard antioxidants and antidiabetic drugs.

Results: The formation of Fe_2O_3 NPs was confirmed by UV-visible spectroscopy, showing a characteristic absorption peak at 440 nm after 48 h. The synthesized nanoparticles exhibited strong antioxidant activity, with DPPH radical scavenging activity ranging from 63.55% to 88.32% at concentrations of 10–50 µg/mL, comparable to the standard ascorbic acid. Significant α-amylase inhibitory activity (48–84%) was observed when compared with the standard drug acarbose. Overall, the results demonstrated concentration-dependent antioxidant and antidiabetic efficacy of the biogenically synthesized iron oxide nanoparticles.

Conclusion: The biogenic synthesis of iron oxide nanoparticles using *H. umbellata* L. is an eco-friendly and cost-effective approach. The synthesized nanoparticles exhibited excellent antioxidant and antidiabetic activities, highlighting their potential as promising candidates for the development of plant-based nanotherapeutics.

Keywords: Antioxidant activity, Antidiabetic activity, Biosynthesis, *Hydrocotyle umbellata* L, Iron oxide nanoparticles.

 DOI: http://dx.doi.org/10.22159/ajpcr.2026v19i4.58004. Journal homepage: https://innovareacademics.in/journals/index.php/ajpcr

INTRODUCTION

The family Araliaceae, to which *Hydrocotyle umbellata* L. belongs, is widely distributed in South Asia, particularly in India and China, as well as in Argentina and Brazil [1]. *H. umbellata* L. has been traditionally used in Ayurvedic medicine due to its anxiolytic and memory-enhancing properties. Previous studies have reported its therapeutic potential in the treatment of skin disorders, rheumatism, splenic ailments, tuberculosis, hypertension, hepatic conditions, and gastrointestinal disorders [2].

Green synthesis of nanoparticles has gained significant attention as an alternative to conventional chemical methods, the plants derived phytochemical as cost-effective, natural reducing, stabilizing agents, improving biocompatibility, environmentally benign, and eliminate the use of toxic reducing agents [3]. Matter exists across multiple length scales, ranging from macroscopic objects visible to the naked eye to microscopic entities such as cells and microorganisms that require optical instruments for observation. Bridging these dimensions are nanomaterials, which typically possess sizes between 1 and 100 nm and exhibit unique physicochemical properties [4].

Nanotechnology has revolutionized various industrial and biomedical sectors owing to the high surface-to-volume ratio and enhanced reactivity of nanomaterials. However, traditional nanoparticle synthesis methods employing chemicals such as sodium borohydride raise significant environmental and health concerns. Consequently, biological sources, particularly plant extracts, have emerged as sustainable alternatives for nanoparticle synthesis [5,6].

Metal nanoparticles, especially iron oxide nanoparticles (Fe_2O_3 nanoparticles [NPs]), have been extensively explored for biomedical applications due to their remarkable chemical and physical characteristics. Fe_2O_3 NPs are highly reactive and have been utilized in magnetic resonance imaging and hyperthermia-based cancer therapy [7,8]. In addition, biosynthesized Fe_2O_3 NPs exhibit notable free radical scavenging activity, thereby enhancing the body's natural antioxidant defense mechanisms. Their catalytic efficiency has been reported to be significantly higher than that of conventional materials [9].

Oxidative stress, resulting from an imbalance between reactive oxygen species (ROS) production and antioxidant defenses, plays a critical role in the pathogenesis of several diseases and the aging process [10]. ROS are continuously generated through normal cellular redox reactions, and excessive accumulation can lead to cellular damage, thereby accelerating aging and disease progression [11]. Therefore, the present study aims to biosynthesize iron oxide nanoparticles using H. umbellata L. and to evaluate their antidiabetic activity for utilizing the alpha amylase and alpha glucosidase technique and free radical scavenging activity for utilizing the 2,2-diphenyl-1-picrylhydrazyl

(DPPH) assay, H_2O_2 assay, Ferric reducing antioxidant powers (FRAPs) analysis, 2,2'-azino-bis(3-ethylbenzothiazoline-6-sulfonic acid) (ABTS) technique, and nitric oxide analysis.

METHODS

The following instruments were used in the present study such as orbital shaker (Lark), magnetic stirrer (Remi), and double beam ultraviolet (UV)-visible spectrophotometer-2377. Samples were uniformly stirred using an orbital shaker (Lark). In order to provide adequate mixing and improve mass transfer in the liquid medium, the device moves samples in a circular motion at a regulated speed. Liquid samples were continuously mixed using a magnetic stirrer (Remi). By spinning a magnetic bar inside the container, the apparatus preserves solution homogeneity, which is necessary for reliable experimental results and constant reaction conditions. Then, using a double beam UV-spectrophotometer (model 2377). The instrument measures absorbance by comparing the intensity of light passing through the sample.

H. leumbellata L. extract preparation

The *H. umbellate* L. plant was gathered from the Nanoherbo Garden of Saveetha Medical College and Hospital, Chennai. The plant was rinsed with tap water for 3 times because the removal of dust particles. The washed plant was cut into small pieces, and the pieces were dried into the sunshade for 4 days at 35°C. The dried plant was ground into fine powder, and 1 g of *H. umbellata* powder was mixed with 100 mL of distilled water. The mixed plant powder solution was placed in the heating mantle for 20 min at 50–60°C. The boiled extract was filtered and stored at 4°C for further utilization in research. The herbal extract was utilized for the phytofabrication of a nanoparticle solution.

Preparation of Fe_2O_3 NPs

The phytofabrication of iron oxide nanoparticles was utilized for a 30 millimolar $FeCl_3$ solution and mixed with 50 mL of *H. umbellata* extract. The mixed solution was placed in the orbital shaker for 48 h, the color changes were observed, and any precipitate formation was also noted. Every 12 h, the UV-visible spectroscopy, and the maximum absorbance peak was noted. The synthesized nanoparticle was centrifuged at 8000 rpm for 10 min. The collected pellet was utilized for further research and analyzed for its biomedical applications.

Characterization

The green synthesized iron oxide nanoparticle was analyzed for the functional group in Fourier transform infrared spectroscopy (FTIR) analysis, the crystalline structure and amorphous nature were analyzed in X-ray diffraction (XRD) analysis, and the structure of the nanoparticles was done by scanning electron microscopy (SEM) analysis.

Antidiabetic assays

Determination of alpha-amylase enzyme inhibition

To prepare the enzyme solution, this assay was followed by previous research work [12], 100 mg of alpha amylase was dissolved in 10 mL of dis H_2O. 100 mL of alpha amylase was added, and various concentrations of iron oxide nanoparticle solution (10–50 µg/mL). The solution was placed in the incubator for 30 min at 37°C. After the completion of incubation, prepared 1% starch solution was prepared. 100 mL of starch solution was added in the tubes. The solution was placed in the incubated for 10 min at 37°C. After that, 100 mL of 3,5-dinitrosalicylic acid (DNSA) was added, and the tubes were measured for absorbance at 540 nm for utilizing the colorimetric analyzer. The standard was utilized for Acarbose.

Evaluation of the alpha-glucosidase enzyme inhibition

To prepare the enzyme solution, 100 mg of alpha-glucosidase was dissolved in 10 mL of distilled water. 100 mL of alpha amylase was added, and various concentrations of iron oxide nanoparticle solution (10–50 µg/mL). The solution was placed in the incubated for 30 min at 37°C. After the completion of incubation, prepared 1% starch solution was prepared. 100 mL of starch solution was added to the tubes. The solution was placed in the incubated for 10 min at 30°C. After that, 100 mL of DNSA was added, and the tubes were measured for absorbance at 540 nm for utilizing the colorimetric analyzer. The standard was utilized for Acarbose.

Antioxidant activity

DPPH radical scavenging assay

To analyze the free radical scavenging for iron oxide nanoparticles utilizing the DPPH analysis. 200 mL of 2% DPPH (0.1 mM) solution was added, and various concentrations of iron oxide nanoparticles (10–50 µg/mL). The tubes were placed in the dark incubation for 10 min at 37°C. After the completion of incubation, the tubes were measured at an absorbance of 517 nm utilizing the colorimetric analyzer. The standard was utilized as ascorbic acid and control as dimethyl sulfoxide (DMSO).

Hydrogen peroxide radical scavenging assay

To analyze the free radical scavenging for iron oxide nanoparticles utilizing the DPPH analysis. 200 mL of 2% H_2O_2 solution was added, and various concentrations of iron oxide nanoparticles (10–50 µg/mL). The tubes were placed in the dark incubation for 10 min at 37°C. After the completion of incubation, the tubes were measured at an absorbance for 532 nm utilizing the colorimetric analyzer. The standard was utilized as ascorbic acid and the control as DMSO.

FRAP assay

FRAP reagents

a) To prepare the acetate buffer 300 mM pH 3.6, weigh 3.1 g sodium acetate trihydrate, add 16 mL glacial acetic acid, and dilute with 1 L of distilled water
b) 2, 4, 6-tripyridyls-triazine: (MW 312.34), 10 mM in 40 mMHCl (MW 36.46)
c) $FeCl_3$. 6 H_2O: (MW 270.30), 20 mM. Just before testing, the functioning FRAP reagent was made by mixing a, b, and c in a 10:1:1 ratio. The standard was $FeSO_4$. 7 H_2O: 0.1–1.5 mM in methanol.

Assay

The iron oxide nanoparticle was added at various concentration (10–50 µg/mL), and mixed with FRAP reagent. The tubes were incubated for 10 min at 37°C and the tubes were observed for color changes. After that, the tubes were measured at 720 nm to utilize the colorimetric analyzer.

ABTS assay

ABTS analysis of free radical scavenging, this assay was followed by the previous research articles [13]. It was reacting with iron oxide nanoparticles (10–50 µg/mL), and the standard was utilized with ascorbic acid.

Nitric oxide radical inhibition assay

10 mM of sodium nitroprusside solution, 500 mL of ×10 phosphate buffered saline buffer solution, and various concentrations of iron oxide nanoparticle (10–50 µg/mL). The tubes were incubated for 30 min at 30°C. The prepared Griess reagent, 0.5 mL of Griess reagent, was added to the tubes. The test tubes were incubated for 30 min, and the pink color was observed in the tubes; the tubes were measured at 546 nm.

Statistical analysis

The green synthesis of iron oxide nanoparticles using *H. umbellata* in each assay was repeated for 3 times (n=3) and the data was utilized the statistical tool Graphpad version 8.0, Data were analyzed the TWO-WAY analysis of variance and multiple comparisons between the groups were carried out utilizing Turkey's test.

RESULTS

The biogenesis of iron oxide nanoparticles using *H. umbellata* L. plant extract was initially confirmed by UV-visible spectroscopic analysis,

where the Y-axis is absorbance (−0.5–3.0), and the X-axis is wavelength (250–650 nm).After 48 h of incubation, the UV-Vis spectrum exhibited a distinct absorbance peak (range 250–650 nm) at 440 nm and the absorbance was 1.403, indicating the preliminary confirmation of the development of iron oxide nanoparticles (Fig. 1a), and the plant extract (*H. umbellate)* was taken with the UV-reading at 435 nm and the absorbance was 2.284. Following confirmation, the nanoparticle suspension was centrifuged at 8,000 rpm for 10 min. The resulting pellet was collected and subsequently used for further characterization and evaluation of biomedical applications.

The XRD analysis of iron oxide nanoparticles showed the 32.6% crystalline in nature and amorphous in 67.4%, the maximum peak as 29.74°, 31.66°, 32.31°, 41.35°, 44.89°, 49.74°, 51.21°, 67.52°, and 74.03°. The HK1 value of the iron oxide nanoparticles as (012), (104), (104), (113), (202), (024), (116), (300), (1010) Fig. 1b, respectively.

The morphology of the synthesized iron oxide nanoparticles was determined using SEM analyses. The iron oxide nanoparticles showed the morphology analysis as irregular spherical analysis in various sizes as 2 μm and 500 nm (Fig. 2a and b). FTIR analysis was carried out to determine the green synthesis of iron oxide nanoparticles, including bonding and stretching vibration. In the peak was observed and showed as 3261 cm^{-1} in O-H bonding, 2923 cm^{-1} as very strong carboxylic acid O-H stretching, 1609 cm^{-1} as C=C stretching alkene group, 1435 cm^{-1} C-H bending as alkane, 1028 cm^{-1} as C-F stretching in fluoro compound, and 800.04 cm^{-1} as C=C bending in alkene group (Fig. 2c). These are the functional groups that were presented in the iron oxide nanoparticles.

Antioxidant activity

In DPPH showed the inhibitory percentage of the iron oxide nanoparticles as various fixations as (10–50 μg/mL) as 63.55–88.32% and the ascorbic acid revealed the inhibitory % as 66.25–93.15% (Fig. 3a). Fig. 3b, In H_2O_2 assay revealed the outcomes as lower range of iron oxide nanoparticle as 10 μg/mL as 48.5% and the standard as 51.1%, and the higher fixation as 50 μg/mL as 86.3 and 89.9% of inhibition. In FRAP assay, the iron oxide nanoparticles showed the inhibitory percentage as compared with standard (ascorbic acid) in 70.26% and 72.98% in the least concentration of nanoparticles (Fig. 3c). Both inhibitory percentages were very similar and it showed the effective antioxidant potential. As shown in Fig 3d, ABTS analysis revealed the outcomes as 66.89%, 73.69%, 80.45%, 82.16%, and 88.33% and the standard as 70.56%, 75.68%, 82.43%, 86.57%, and 91.39%. In nitric oxide assay, the iron oxide nanoparticles was showed the concentrations level as gradually increased and inhibitory % also increased as 10 μg/mL in 68.35%, 50 μg/mL in 86.12%, and the ascorbic acid showed the 72.43–88.67% (Fig. 3e).

Anti-diabetic activity

In anti-diabetic activity was done by using the iron oxide nanoparticles using the *H. umbellata*, in alpha amylase showed the inhibitory percentage of iron oxide nanoparticles as (10–50 μg/mL) in (48–84%) (Fig. 4a). The IC_{50} values were also revealed as 8.20 μg/mL and the standard as 5 μg/mL, in concentration of nanoparticles was raised, and the % of inhibition also raised. Fig. 4b, In alpha-glucosidase, as revealed by the inhibitory percentage, the percentage was higher at a higher concentration (50 μg/mL) 83% and the standard was 89% and the IC_{50} as 4.6 μg/mL in Fe_2O_3 NPs and 2.6 in standard.

DISCUSSION

In previous research, iron oxide nanoparticles were utilized for *Borassus flabellifer* and it was confirmed that the synthesis of the maximum absorbance peak was recorded at 352 nm [14]. In a similar study, the biogenesis of Fe_2O_3 NPs using the *Ulva lactuca* showed the UV peak at 325 nm using the UV spectroscopy for the analysis of synthesized nanoparticles [15].

In other research work, in FTIR analysis was analyzed the functional group of the nanoparticles, it was revealed as some peaks at 3272, 2922,

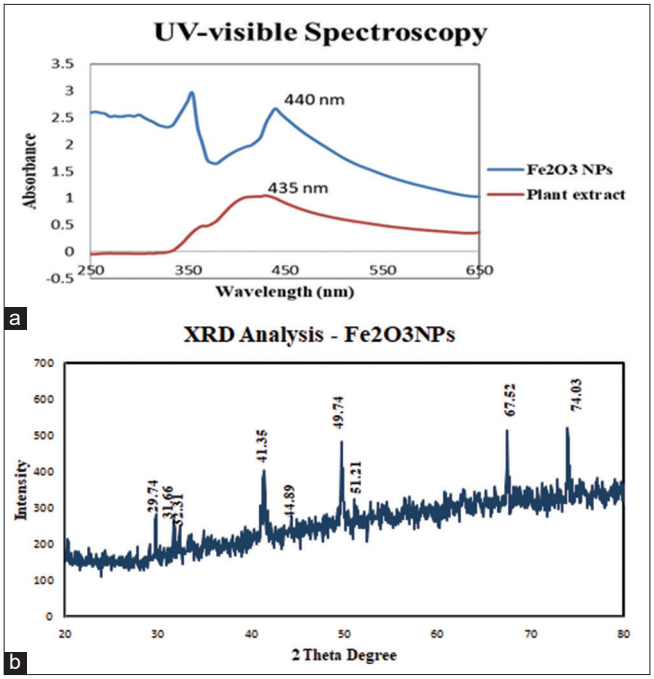

Fig. 1: (a) Ultraviolet-visible absorption spectrum of *umbellata*-mediated iron oxide nanoparticles showing a characteristic peak at 440 nm, indicating successful biosynthesis and (b) the X-ray diffraction analysis of iron oxide nanoparticles

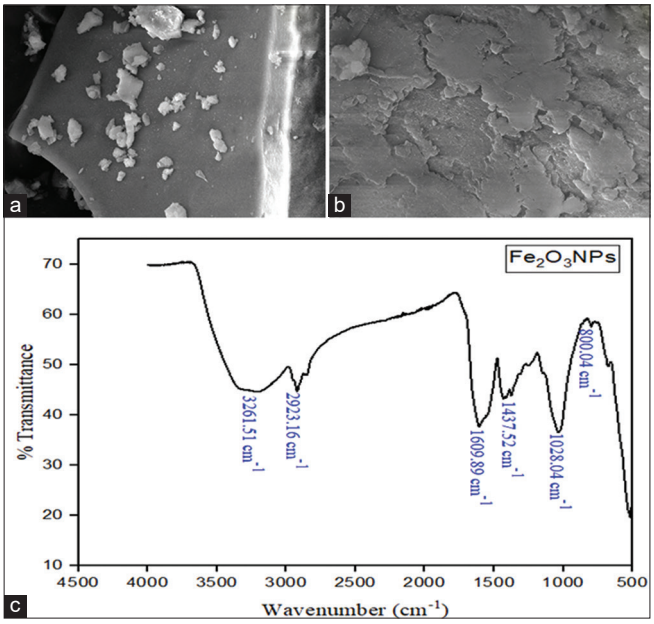

Fig. 2: The image represented the scanning electron microscopy (SEM) analysis and fourier transform infrared spectroscopy (FTIR) analysis of iron oxide nanoparticles. (a) 2 μm, 5.00 KX Magnification of iron oxide nanoparticles, and (b) 500 nm, 20.00 KX Magnification of iron oxide nanoparticles, (c) FTIR analysis of *Hydrocotyle umbellate* mediated iron oxide nanoparticle

1632, 1520, 1453, 1379, 1222, and 1051 cm^{-1} and the functional groups as O-H (hydrogen bonded) as alcohol group, O-H as carboxylic acid, C-H bending as aromatic compound, N-O stretching as nitro compound, C-H as alkane group, C-H bonding as aldehyde group, C-F stretching as fluoro compound, and C-O as primary alcohol group was found [16]. In similar study, the FTIR analysis of iron oxide nanoparticles was showed the absorbance peak at the range as 400–3900 cm^{-1}, 3906.27

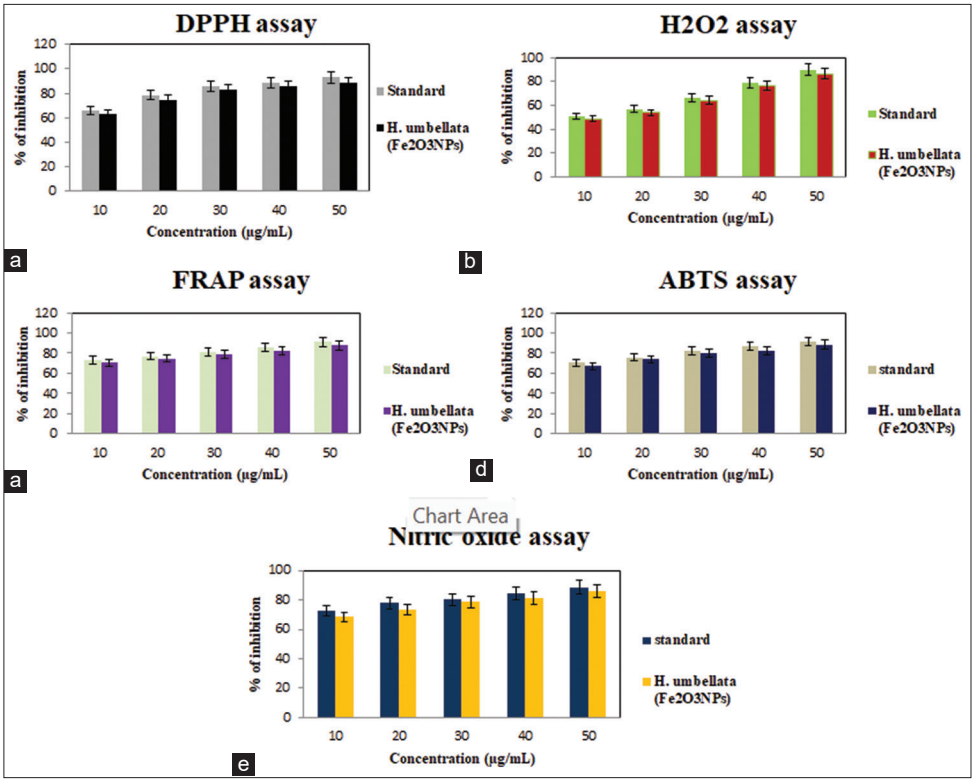

Fig. 3: Graphical presentation dose-dependent, antioxidant activity of biosynthesized Fe_2O_3 nanoparticles and ascorbic acid (standard). (a) 2,2-Diphenyl-1-picrylhydrazyl radical scavenging, (b) H_2O_2 scavenging, (c) Ferric reducing antioxidant power reducing power, (d) 2,2'-azino-bis(3-ethylbenzothiazoline-6-sulfonic acid)$^+$ radical scavenging, (e) Nitric oxide radical inhibition and the statistical significance with the p-values as ***p<0.0001

and 483.93 cm^{-1} as the function group 3906.27 as (O-H bonding) alcohol and phenolic group, and M-O stretching as metal-oxygen (inorganic group) was presented [17]. In previous research work, the green synthesis of iron oxide nanoparticles from *Iris kashmiriana* was showed the morphology as 20–40 nm as twisted hexagon shape [18]. *Argemone mexicana* mediated iron oxide nanparticles was analsized the morphological as 5, 2, and 1 µm. It was shown that the predominantly hexagonal and irregular shape was observed [19]. In previous research work, the green synthesis of iron oxide nanoparticles at 2 theta degree as 30.2°, 35.5°, 43.2°, 53.8°, and 57.3°, and the matched as (220), (311), (400), (422), and (511) of Fe_2O_3 NPS of crystals [20]. In similar study, the green synthesis of iron oxide nanoparticles and the X-ray diffraction spectrum of the nanoparticles as the 2 theta degree as 33.16°, 35.56°, 40.87°, 49.43°, 53.96°, 62.46°, and 64.02° are assigned to (104), (110), (113), (024), (116), (214), and (300), respectively [21].

In antioxidant activity, *Coleus amboinicus* was used to synthesize the iron oxide nanoparticles. In DPPH assay was revealed the inhibitory percentage as (65.8%–89.7%) and the standard as (66.23–93.15%) in various concentrations of iron oxide nanoparticles (10–50 µg/mL) [22] and the DPPH solution was purple in color, it was react with nanoparticles and converted into yellow color solution. The reduction process, DPPH, was reducing the electron and the reflected as color changes and observed in 517 nm [23]. In similar concentration for FRAP assay in the inhibitory percentage as (66.4–90.7%) [24]. The mechanism of the FRAP assay, whereas reducing the ferric into ferrous at the low pH (3.6) and the indication of color changes as visual observed and measured at 720 nm in colorimetric analysier [25]. In similar work, *Phoenix dactylifera* extract-based fabrication of iron oxide nanoparticles showed the antioxidant efficacy as various fixations at (0.03, 0.02, and 0.01) [26]. In previous research work, *Thymus migricus* was utilized to synthesized the iron oxide nanoparticles as revealed the DPPH inhibitory percentage at the range of 25–200 mg/L and the inhibitory percentage as 38.6–75.4%) [27,28].

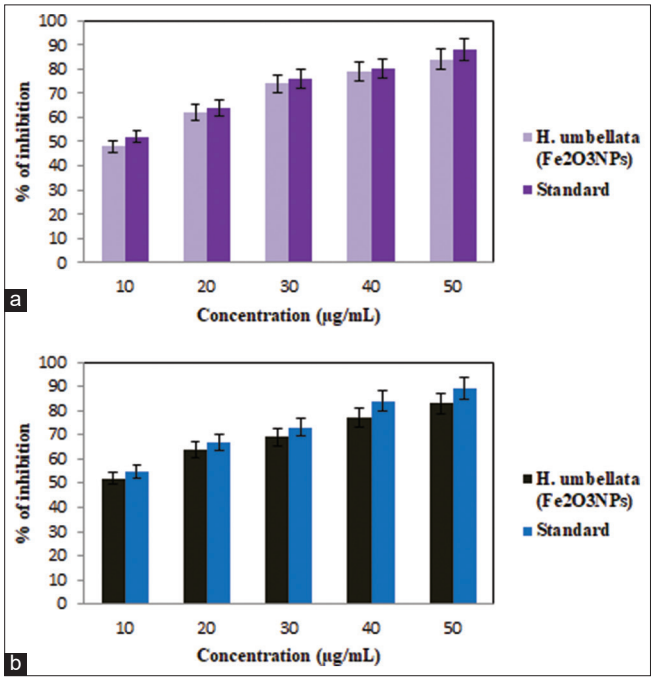

Fig. 4: Inhibitory effect of biosynthesized Fe_2O_3 nanoparticles and acarbose (standard) on (a) alpha-amylase and (b) alpha-glucosidase enzymes

In another study of research work, the mechanism of anti-diabetic activity was used as alpha glucosidase enzyme as catalyze, which involved a hydrolysis process that converted disaccharides and polysaccharides into glucose. It was reduce the postprandial blood glucose level [29].

In previous research, *Gongronema latifolium* as aqueous extract was used to synthesize the Fe_2O_3 NPs and it's evaluated the anti-diabetic activity as alpha amylase, showing the inhibitory percentage at the various fixations as (50–500 µg/mL) as 96.320 µg/mL [30]. In similar study, biogenesis of Fe_2O_3 NPs using *Madhuca indica* and the alpha amylase showed the inhibitiory percentage as 32.1–73.3% and the concentrations as 200–1,000 µg/mL, In alpha amylase enzyme that was hydrolyze the alpha 1,4- glycosidic bond it breaks down the starch (reduce the carbohydrate) and preventing the blood sugar level. The reaction was stopped down as DNSA and measured at 540 nm in a colorimetric analyzer [31].

CONCLUSION

In the present study, iron oxide nanoparticles were successfully synthesized using H. umbellata L. through a biogenic approach, which significantly reduced chemical usage, environmental pollution, and synthesis time. A concentration-dependent increase in inhibitory activity was observed, with higher concentrations showing greater inhibition. Overall, the iron oxide nanoparticles exhibited strong antioxidant potential in the DPPH assay and effective anti-diabetic activity against the α-amylase enzyme, highlighting their potential for biomedical applications. These results demonstrate the potential of iron oxide nanoparticles mediated by *H. umbellata* as promising nanomaterials for the treatment of metabolic diseases associated with diabetes and oxidative stress. For greater understanding of the underlying molecular mechanisms controlling enzyme inhibition and antioxidant effect, more research is necessary. In order to evaluate bioavailability, safety, and therapeutic efficacy, future research should concentrate on thorough mechanistic investigations, nanoparticle–biomolecule interactions, and *in vivo* validation using suitable diabetic animal wound healing models. Translating these green-synthesised nanoparticles into clinically beneficial nanotherapeutic utilizes involves such investigations.

ETHICAL APPROVAL

No animal or human sample was included in this research article.

CONSENT TO PARTICIPATE

Not applicable.

CONSENT TO PUBLISH

Not applicable.

AVAILABILITY OF DATA AND MATERIALS

No data availability.

ACKNOWLEDGMENTS

We would like to thank Saveetha Institute of Medical and Technical Sciences for support.

AUTHORS CONTRIBUTIONS

Sulochana Govindharaj and Kanish S: Writing – original draft, Validation, Methodology, Investigation, Formal analysis, Data curation. Validation, Methodology, and editing with review of the manuscript, Data curation, and Visualization. Rajeshkumar Shanmugam: Writing – review and editing, Validation, Supervision, Methodology. Kohila Kalimuthu: Investigation, Data curation, Conceptualization.

CONFLICT OF INTEREST

Authors do not have any conflict of interests to declare.

FUNDING

The author does not declare any funding.

REFERENCES

1. Florentino IF, Nascimento MV, Galdino PM, De Brito AF, Da Rocha FF, Tonussi CR. Evaluation of analgesic and anti-inflammatory activities of *Hydrocotyle umbellata* L., Araliaceae (acariçoba) in mice. An Acad Bras Cienc. 2013;85(3):987-97. doi: 10.1590/S0001-37652013000300011, PMID 24068088
2. Oliveira TL, Morais SR, Sá S, Oliveira MG, Florentino IF, Silva DM. Antinociceptive, anti-inflammatory and anxiolytic-like effects of the ethanolic extract, fractions and hibalactone isolated from *Hydrocotyle umbellata* L. (Acariçoba) - Araliaceae. Biomed Pharmacother. 2017;95:837-46. doi: 10.1016/j.biopha.2017.08.140, PMID 28903179
3. Gottimukkala KS, Harika RP, Zamare D. Green synthesis of iron nanoparticles using green tea leaves extract. J Nanomed Biother Discov. 2017;7(1):151.
4. Pattanayak M, Nayak PL. Ecofriendly green synthesis of iron nanoparticles from various plants and spices extract. Int J Plant Anim Environ Sci. 2013;3(1):68-78.
5. Roy A, Singh V, Sharma S, Ali D, Azad AK, Kumar G. Antibacterial and dye degradation activity of green synthesized iron nanoparticles. J Nanomater. 2022;2022(1):3636481. doi: 10.1155/2022/3636481
6. Rajeshkumar S, Malarkodi C, Venkat Kumar S. Synthesis and characterization of silver nanoparticles from marine brown seaweed and its antifungal efficiency against clinical fungal pathogens. Asian J Pharm Clin Res. 2017;10:190-3.
7. Asha S, Asha A, Rajeshkumar S. Evaluation of phytochemical constituents and antimicrobial activity of silver nanoparticle synthesized ipomoea nil against selected pathogens. Asian J Pharm Clin Res. 2017;10:183-7.
8. Begum A, Jeevitha M, Preetha S, Rajeshkumar S. Cytotoxicity of iron nanoparticles synthesized using dried ginger. J Pharm Res Int. 2020;32:112-8. doi: 10.9734/jpri/2020/v32i2530829
9. Mohamed NF, Jeevitha M, Rajeshkumar S, Preetha S. Free radical scavenging activity of iron nanoparticles synthesized using dried ginger. Int J Pharmacol Res. 2020;12(4):3252.
10. Jomova K, Raptova R, Alomar SY, Alwasel SH, Nepovimova E, Kuca K. Reactive oxygen species, toxicity, oxidative stress, and antioxidants: Chronic diseases and aging. Arch Toxicol. 2023;97(10):2499-574. doi: 10.1007/s00204-023-03562-9, PMID 37597078
11. Flieger J, Flieger W, Baj J, Maciejewski R. Antioxidants: Classification, natural sources, activity/capacity measurements, and usefulness for the synthesis of nanoparticles. Materials (Basel). 2021;14(15):4135. doi: 10.3390/ma14154135, PMID 34361329
12. Rajkumar M, Davis Presley SI, Thiyagarajulu N, Girigoswami K, Janani G, Kamaraj C. Gelatin/PLA-loaded gold nanocomposites synthesis using *Syzygium cumini* fruit extract and their antioxidant, antibacterial, anti-inflammatory, antidiabetic and anti-Alzheimer's activities. Sci Rep. 2025;15(1):2110. doi: 10.1038/s41598-024-84098-5, PMID 39814774
13. Rajkumar M, Presley SD, Begum MY, Alamri A, Al Fatease A, Girigoswami K. Biogenic synthesis of CuO-TiO_2 nanocomposites from *Senna auriculata* (L.) Roxb. Plant extract and its evaluation of antioxidant, antibacterial and anticancer activity of HepG2 cell lines. Biocatal Agric Biotechnol. 2025;69:103787.
14. Sandhya J, Kalaiselvam SJ. Biogenic synthesis of magnetic iron oxide nanoparticles using inedible *Borassus flabellifer* seed coat: Characterization, antimicrobial, antioxidant activity and *in vitro* cytotoxicity analysis. Mater Res Express. 2020;7(1):015045. doi: 10.1088/2053-1591/ab6642
15. Bensy AD, Christobel GJ, Muthusamy K, Alfarhan A, Anantharaman P. Green synthesis of iron nanoparticles from *Ulva lactuca* and bactericidal activity against enteropathogens. J King Saud Univ Sci. 2022;34(3):101888. doi: 10.1016/j.jksus.2022.101888
16. El-Sheekh MM, Shaaban MT, Goda A, Morsi HH. Green synthesis of iron oxide nanoparticles using *Lyptolyngbya foveolarum* and *Azospirillum brasilense* for wastewater treatment. Int J Environ Sci Technol. 2025 Jan 04;22:9933-48.
17. Naik H, Manoharadas S, Bommayasamy N, Thomas J, Gobi M, Dewala SR. Green synthesis of iron oxide nanoparticles using *Bacillus subtilis* to mitigate salinity stress in rice (*Oryza sativa* L.) Plants and enhance physiological activities. Environ Sci Nano. 2025;12(4):2421-35. doi: 10.1039/d4en01184h
18. Imtiyaz A, Singh A, Bhardwaj A. Green synthesis of iron oxide nanoparticles from *Iris kashmiriana* (Mazar-Graveyard) Plant extract its characterization of biological activities and photocatalytic activity. J Ind Eng Chem. 2025 Mar 25;143:538-51. doi: 10.1016/j.jiec.2024.09.004

19. Nughwal A, Bharti R, Thakur A, Verma M, Sharma R, Pandey A. Green synthesis of iron oxide nanoparticles from Mexican prickly poppy (*Argemone mexicana*): Assessing antioxidant activity for potential therapeutic use. RSC Adv. 2025;15(13):10287-97. doi: 10.1039/d4ra07232d, PMID 40206387
20. Kiwumulo HF, Muwonge H, Ibingira C, Lubwama M, Kirabira JB, Ssekitoleko RT. Green synthesis and characterization of iron-oxide nanoparticles using *Moringa oleifera*: A potential protocol for use in low and middle income countries. BMC Res Notes. 2022;15(1):149. doi: 10.1186/s13104-022-06039-7, PMID 35468836
21. Aida MS, Alonizan N, Zarrad B, Hjiri M. Green synthesis of iron oxide nanoparticles using *Hibiscus* plant extract. J Taibah Univ Sci. 2023;17(1):2221827. doi: 10.1080/16583655.2023.2221827
22. Kunjan F, Shanmugam R, Govindharaj S. Evaluation of free radical scavenging and antimicrobial activity of *Coleus amboinicus*-mediated iron oxide nanoparticles. Cureus. 2024;16(3):e55472. doi: 10.7759/cureus.55472
23. Sao AP, Loksh K, Jain G, Yaduwanshi P. A comparative study of the phytochemical, free radical scavenging and acid neutralizing potential of ethanol, ethyl acetate, chloroform and hydroalcoholic extract of *Ipomoea reniformis* Choisy. Int J Pharm Pharm Sci. 2025;17(12):36-41. doi: 10.22159/ijpps.2025v17i12.56392
24. Rajeshkumar S, Parameswari RP, Jayapriya J, Tharani M, Ali H, Aljarba NH. Apoptotic and antioxidant activity of gold nanoparticles synthesized using marine brown seaweed: An *in vitro* study. BioMed Res Int. 2022;2022:5746761. doi: 10.1155/2022/5746761, PMID 35872865. Retraction in: BioMed Res Int.
25. Syarifuddin A, Nurrochmad A, Fakhrudin N. GC-MS metabolite profiling, total phenolic, antioxidant activity, and *in silico* approach in chronic anti-inflammatory ethanol extracts of *Polyscias scutellaria* (Burm. F.) Fosberg leaves. Int J Appl Pharm. 2025;17(3):22-9. doi: 10.22159/ijap.2025.v17s3.03
26. Abdullah JA, Salah Eddine LS, Abderrhmane B, Alonso-González M, Guerrero A, Romero A. Green synthesis and characterization of iron oxide nanoparticles by *Pheonix dactylifera* leaf extract and evaluation of their antioxidant activity. Sustain Chem Pharm. 2020;17:100280. doi: 10.1016/j.scp.2020.100280
27. Ashrafi-Saiedlou S, Rasouli-Sadaghiani M, Fattahi M. Green synthesis of iron oxide nanoparticles using *Thymus migricus* for multifunctional applications in antioxidant, antimicrobial, photocatalytic, and seed priming processes. Heliyon. 2025;11(5):e42933. doi: 10.1016/j.heliyon.2025.e42933
28. Sahu R, Shah K. A captivating potential of Schiff bases derivatives for antidiabetic activity. Curr Pharm Des. 2025 Jan;31(1):37-56. doi: 10.2174/0113816128339161240913055034, PMID 39313905
29. Dilipan E, Sivaperumal P, Kamala K, Ramachandran M, Vivekanandhan P. Green synthesis of silver nanoparticles using seagrass *Cymodocea serrulata* (R.Br.) Asch. And Magnus, characterization, and evaluation of anticancer, antioxidant, and antiglycemic index. Biotechnol Appl Biochem. 2023;70(3):1346-56. doi: 10.1002/bab.2444, PMID 36724497
30. Ekozin AA, Isola OB, Inetianbor OC, Omondiale SO, Omojoyegbe RT, Okanlawon TS. Green synthesized iron nanoparticles using *Gongronema latifolium* leaf extract: Characterization, antioxidant, and antidiabetic activities. GVU J Sci Health Technol. 2024;9(1):137-49.
31. Shabbir MA, Naveed M, Rehman SU, Ain NU, Aziz T, Alharbi M. Synthesis of iron oxide nanoparticles from *Madhuca indica* plant extract and assessment of their cytotoxic, antioxidant, anti-inflammatory, and anti-diabetic properties via different nanoinformatics approaches. ACS Omega. 2023;8(37):33358-66. doi: 10.1021/acsomega.3c02744, PMID 37744851